Energy Conversion and Management 304 (2024) 118220

Contents lists available at ScienceDirect

Energy Conversion and Management

journal homepage: www.elsevier.com/locate/enconman

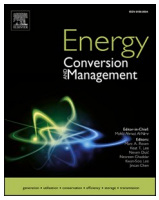

Research Paper

# Power and biogas to methanol – A techno-economic analysis of carbon-maximized green methanol production via two reforming approaches

Stefan Bube *, Lucas Sens, Chris Drawer, Martin Kaltschmitt

*Hamburg University of Technology (TUHH) / Institute of Environmental Technology and Energy Economics (IUE), Eißendorfer Straße 40 21073, Hamburg, Germany*

ARTICLE INFO

*Keywords:*
Methanol
Biogas
Reforming
Process simulation
Methanol production costs
Carbon efficiency

ABSTRACT

The limited potential of sustainably available biomass requires efficient conversion to defossilize future demands of carbon-based chemicals and energy carriers. Therefore, integrating electricity-derived hydrogen into biomass-based production concepts appears promising, maximizing carbon utilization while minimizing biomass requirement. However, specific process concepts and analyses are still lacking to quantify the potential technical and economic benefits of such hybrid production processes. Thus, this research paper investigates this novel approach for decentralized methanol production from biogas within a techno-economic analysis, considering two production configurations. One configuration (BiRef) utilizes electrically heated bi-reforming for syngas generation, while the other configuration (TriRef) uses autothermal tri-reforming. Based on stationary process simulations, in-depth knowledge about process behavior is gained, efficiencies and costs are determined, and influencing factors are assessed. Within the reference case, the BiRef configuration achieves a carbon efficiency of 93 %, while the TriRef configuration reaches 97 % due to its enhanced methane conversion. Energy efficiency is 5 %pt. higher within the BiRef configuration (74 %), primarily due to the lower hydrogen demand. Carbon and energy efficiency are crucially affected by reforming temperature and inert gas fraction in the syngas. The economic analysis shows methanol production costs of ca. 1,300 $€_{2022}$/t for both configurations. Variations in economic parameters emphasize advantages for the TriRef configuration when low hydrogen costs (<6 $€_{2022}$/kg) are achievable. The comparison with purely biogas-based methanol production shows that hydrogen addition increases production capacity by up to 67 %. Cost advantages result against purely electricity-based production, while cost parity is achieved with purely biogas-based production. This paper demonstrates the potential of hybrid methanol production for efficient biogas utilization and highlights decisive parameters influencing technical and economic efficiency.

## 1. Introduction

The imperative necessity of defossilizing the highly industrialized economy to mitigate anthropogenic climate change requires a transformation of all sectors toward the utilization of renewable sources of energy and materials. However, from today's perspective, some sectors, such as the chemical industry and most likely also specific segments within the transportation sector (e.g., long-haul air transport), will persist in their reliance on carbon-based molecules over the long term due to the absence of viable decarbonization alternatives. The non-fossil (so-called "green") production of these substances requires significant amounts of energy from renewable sources and sustainable carbon. The latter is either obtained from biomass or extracted as carbon dioxide from the atmosphere. Due to the comparable low atmospheric concentration (approximately 420 ppm [1]), such a direct air capture (DAC) process requires significantly higher energy and engineering efforts

*Abbreviations: ACC*, Annual capital cost; AFLH, Annual full load hours; BGtM, Biogas-to-Methanol; BiRef, Bi-reforming; *CAPEX*, Capital expenditures; CEPCI, Chemical plant cost index; *COR*, Carbon oxide ratio; CSDR, Combined steam and dry reforming; DAC, Direct air capture; *FCI*, Fixed capital investment; HHV, Higher heating value; IGF, Inert gas fraction; LHV, Lower heating value; *MPC*, Methanol production cost; *OPEX*, Operational expenditures; PBGtM, Power- and Biogas-to-Methanol; PtM, Power-to-Methanol; PV, Parameter variation; RC, Reference case; SG, Syngas; *SN*, Stoichiometric number; TriRef, Tri-reforming; *WACC*, Weighted average cost of capital; WGS, Water-gas shift.

* Corresponding author.
*E-mail address:* stefan.bube@tuhh.de (S. Bube).

https://doi.org/10.1016/j.enconman.2024.118220
Received 5 December 2023; Received in revised form 22 January 2024; Accepted 16 February 2024
Available online 22 February 2024

compared to carbon supply from biomass processing, making these approaches much more expensive [2,3]. However, sustainably available biomass is severely limited due to competition in land use and utilization. Hence, maximizing the utilization of the carbon inventory from biomass needs to be prioritized for efficiency reasons, provided a sustainable origin of the utilized biomass can be ensured.

Sustainable biomass, such as manure or straw, is primarily generated within agriculture. So far, these materials are typically, if at all, utilized energetically – i.e., for electricity and heat production – commonly realized through anaerobic biomass fermentation and biogas combustion. Instead of this most widely realized utilization pathway, biogas – which typically consists mainly of methane ($CH_4$) and carbon dioxide ($CO_2$) – can also be converted into higher-value substances through reforming and subsequent synthesis processes. Due to its selective and small-scale implementable synthesis technology, methanol ($CH_3OH$) is particularly suitable as a target product [4,5]. Methanol is one of the most important organic primary chemicals, with a global (fossil-based) production exceeding 100 Mt/a [6,7]. Thus, "green" methanol can potentially contribute to defossilization within various sectors of the economy [6,8].

Biogas-based methanol production (biogas-to-methanol; BGtM) takes place through syngas production and subsequent conversion into methanol. Depending on the biogas composition and the reforming process, the syngas produced has a greater or lesser hydrogen ($H_2$) deficit compared to the stoichiometric ratio required for methanol synthesis. Conventionally, this deficit can be balanced by $CO_2$ separation, possibly involving an additional water–gas shift (WGS) reaction. However, this is associated with significant carbon losses and an increased relative biogas demand. A novel approach to compensate for the hydrogen deficit and, thus, to maximize carbon utilization is depicted in Fig. 1–1 and involves the addition of "green" $H_2$ produced from "renewable" electricity.[1] The electricity-based $H_2$ production converts electrical energy into chemical energy via water-electrolysis and is predominantly discussed under the general term "power-to-x" (PtX). The combined overall concept (power- and biogas-to-methanol; PBGtM) enables the complete utilization of the biogas carbon potential, consequently reducing the specific biogas demand for methanol production and potentially realizing higher production capacities based on the available biogas quantity.

Concerning the operation of the plant, it has to be taken into account that the availability of renewable electricity used for $H_2$ generation is often volatile due to the characteristics of renewable energy sources like wind power and solar radiation. In contrast, biogas production is a (more or less) stationary process. Additionally, reforming favors steady-state operation due to high temperatures and heat transfer requirements, even when advanced synthesis concepts allow for dynamic methanol syntheses downstream. Thus, to operate such a PBGtM concept, sufficient storage options are required to smooth volatile electricity and/or $H_2$ generation and to enable a constant $H_2$ supply.

In recent years, various studies have been carried out on the synthesis-based conversion of biogas-like gases into higher-value products like methanol. Since dry reforming only allows stoichiometrically complete reforming when the biogas composition is equimolar ($CH_4/CO_2 = 1$) and encounters issues with coke formation, current investigations primarily explore concepts involving additional oxidation agents for reforming (i.e., $H_2O$ for bi-reforming or $H_2O$ and $O_2$ for tri-reforming). Respective techno-economic analyses for bi-reforming-based methanol production from biogas and similar mixtures are available, focusing mainly on the reforming parameters and achievable syngas compositions (e.g., Entesari and Goeppert [9], Acquarola et al. [10,11] and Chein et al. [12]). Tri-reforming of biogas for synthesis product generation has been investigated, also focusing mainly on syngas production (e.g., Hernández and Martín [13], Chein and Hsu [14], Farsi and Lari [15], Zhang et al. [16]). Regarding hybrid methanol production, Lim et al. [17] projected methanol production costs from natural gas and $CO_2$ via tri-reforming in the range of 500 to 850 €/t, considering different electrolysis processes for $H_2$ production. Techno-economic and environmental assessments have also been carried out for methanol production from landfill gas via dry and bi-reforming (Choe et al. [18]). Additionally, Moioli and Schildhauer [19] compared different methanol production concepts from biogas, showing that the additional utilization of $H_2$ potentially enables higher carbon utilization and, therefore, higher productivity. However, a detailed comparison of the mainly discussed reforming technologies within the overall production concept for the carbon-maximized biogas conversion to methanol is missing. Therefore, further investigations are necessary to assess the overall concept of hybrid methanol production from biogas regarding the available reforming technologies and the influence of decisive process and framework parameters.

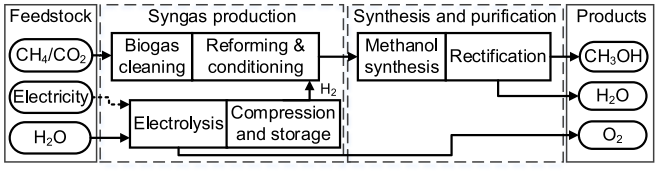


**Fig. 1–1.** Power- and biogas-to-methanol concept.

Against this background, this research paper aims to conduct an in-depth techno-economic assessment of carbon-maximized methanol production from biogas and renewable electricity within a novel decentralized production concept. Two process configurations relying on different reforming technologies are designed and compared to assess the hybrid methanol production concept and evaluate the advantages and disadvantages of the considered reforming technologies within the overall concept. The influence of decisive operating parameters and technical and economic framework conditions are obtained as further novel results. For this purpose, both configurations are modeled using steady-state process simulations. Carbon and energy flow diagrams visualize the simulation results to indicate losses and accumulations. Furthermore, techno-economic key figures are derived and assessed under parameter variation.

The supplementary information provides technical information on the considered process steps and further detailed information about process modeling data, analysis, and results.

## 2. Methodology

The techno-economic analysis of the previously outlined PBGtM concept is conducted based on process modeling results. Within the scope of the analysis, two process configurations, relying on either bi-reforming or tri-reforming (section 3.1), are compared. Fig. 2–1 presents the applied overall assessment approach. The respective tools and methodologies used are described below.

### 2.1. Process design and simulation

The design and the simulation of the process configurations form the basis of the analysis and the assessment.

#### 2.1.1. Process design

Two process configurations are designed according to the general concept of PBGtM, differing regarding the reforming technologies considered: the bi-reforming (BiRef) and tri-reforming (TriRef) of biogas. Preferably, only technically mature technologies or at least technologies that have been extensively investigated and for which

[1] Refers in this work always to electricity generated from renewable sources of energy.

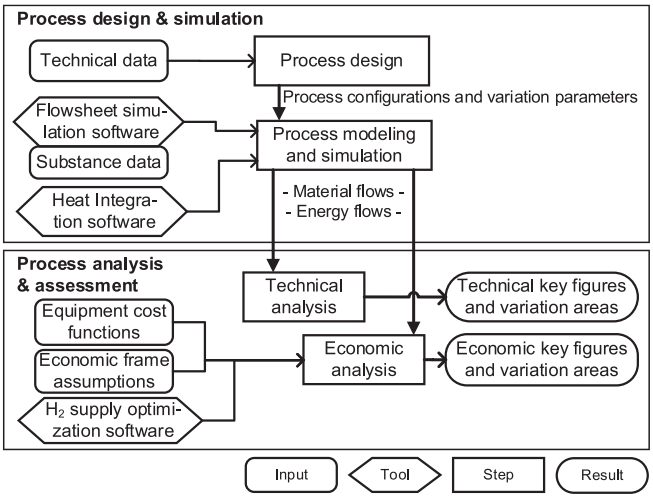


**Fig. 2–1.** Assessment approach of the techno-economic analysis.

sufficient literature data are available are selected. Parameters for which a significant influence on the overall processes can be expected and/or for which literature shows large value ranges are identified and varied within the simulation (parameter variation). Due to the stationary operating characteristics of biogas plants and the limited dynamics of the biogas reforming step, hydrogen production is designed for a constant supply [20].

#### 2.1.2. Process modeling and simulation

A steady-state flowsheet simulation is used to determine the mass and energy flows in the analyzed processes. The commercial simulation software Aspen Plus® is used to determine the occurring material and energy streams. Details about the included methodology, simulation structure, and software databases are provided by [21]. The respective process blocks are interconnected through material, heat, or power streams. Simulation results are used to make iterative adjustments to the process design, optimizing the overall process within the expected technical limitations. No internal integration of heat streams is assumed at this stage. Minimal external heating and cooling requirements are determined via a pinch analysis using the Aspen Energy Analyzer®.

### 2.2. Process analysis and assessment

For both process configurations, a reference case (RC) as well as various technical and economic parameter variations (PV) are analyzed. The ranges of parameter variation are determined based on literature and simulation data to assess the extent of potential deviations from the reference case. The analysis includes the technical and economic key figures described in the following.

#### 2.2.1. Technical analysis

The derived mass and energy balances are visualized for the technical analysis regarding carbon and energy flows, enabling a comprehensive understanding of the overall process schemes. The technical key figures carbon and energy efficiency are defined according to Eq. 2–1 and Eq. 2–2.

Carbon efficiency ($\eta_C$) describes the amount of carbon bound in the target product ($\dot{C}_{\text{Product}}$) compared to the amount of carbon contained within the feedstock ($\dot{C}_{\text{Feed}}$) by considering the respective carbon flows. Since methanol is the only carbon-containing product within the investigated concept, carbon efficiency directly correlates with the methanol production rate.

$$\eta_{\text{C, Product}} = \frac{\dot{C}_{\text{Product}}}{\dot{C}_{\text{Feed}}} \tag{2–1}$$

Energy efficiency ($\eta_{\text{e,Product}}$) is used to assess the process configurations regarding their overall energy demands. The chemical energy of the product is related to the energetic effort of production, considering the chemical energy of the feedstock plus the demand for electrical energy ($P_{\text{el}}$) and thermal process energy ($\dot{Q}_{\text{th}}$). Chemical energy is calculated by multiplying the mass flow of the respective product ($\dot{m}_{\text{Product}}$) or feed ($\dot{m}_{\text{Feed}}$) with the respective higher heating value (HHV).

$$\eta_{\text{e, Product}} = \frac{\dot{m}_{\text{Product}}\text{HHV}_{\text{Product}}}{\dot{m}_{\text{Feed}}\text{HHV}_{\text{Feed}} + P_{\text{el}} + \dot{Q}_{\text{th}}} \tag{2–2}$$

#### 2.2.2. Economic analysis

The primary objective of the economic analysis is to derive and compare methanol production cost (*MPC*) from the analyzed process configurations under defined economic framework conditions. The *MPCs* represent the minimum required selling prices to achieve economic feasibility in methanol production. The costs are calculated according to Eq. 2–3 for a market-mature process ($n^{\text{th}}$-of-a-kind plant) built on a green field. The *MPCs* consist of the annual capital costs (*ACC*), the fixed operational expenditures ($OPEX_f$) and the variable operational expenditures ($OPEX_v$). The latter represent the feedstock and energy costs, while the fixed operational expenditures are independent of the product amount (e.g., labor, taxes, overheads, maintenance). The overall annual costs are related to the annual production given by the hourly nominal production ($\dot{m}_{\text{Product}}$) and annual full load hours (*AFLH*) of the plant.

$$MPC = \frac{ACC + OPEX_f + OPEX_v}{\dot{m}_{\text{Product}}\, AFLH} \tag{2–3}$$

The annuity method (Eq. 2–4) is used to determine the annual capital cost (*ACC*). The capital required for the construction of the plant (fixed capital investment; *FCI*) is depreciated over the depreciation period ($n$), taking into account the real weighted average cost of capital (*WACC*, $i$) and the working capital share ($\omega$).

$$ACC = FCI\,\frac{i\,(1+i)^n}{(1+i)^n - 1} + FCI\,\omega\,i \tag{2–4}$$

The *FCI* is derived using the module costing technique, which is generally accepted as an approach for preliminary cost estimates [23]. This estimate is based on the major process equipment, which is roughly dimensioned based on the process design and simulation. This cost calculation method can be classified as a study estimate[2] with an expected accuracy range of −30 to + 50 % [22]. Detailed calculation principles and assumptions are described in the supplementary information.

Since constant hydrogen supply from volatile energy sources requires dimensioning based inter alia on representative renewable energy production profiles, hydrogen supply costs are derived using hydrogen supply optimization methodology [20], aiming to minimize the hydrogen supply cost by scaling the individual process steps. Hydrogen costs are considered as $OPEX_v$ and derived for a production in Germany.

## 3. Process configurations

The following describes the designed PBGtM process configurations (BiRef and TriRef) and the assumed data and framework conditions.

### 3.1. Process description

The two considered process configurations are listed in Table 3–1.

[2] Also known as Major Equipment Estimate; Estimation Class 4 according to AACE Recommended Practice No. 17R-97.

**Table 3–1**
Process configurations considered.

| Configuration abbreviation | Reforming technology | Heat provision |
|---|---|---|
| BiRef | Bi-reforming | Electrical heated |
| TriRef | Tri-reforming | Autothermal |

- BiRef. Combining steam reforming and dry reforming (CSDR), the bi-reforming process appears to be significantly advantageous over dry reforming, particularly concerning coke formation and product composition [23]. Instead of a fired reactor system, conventionally used for endothermic reforming processes, an electrically heated reformer is considered to avoid carbon losses related to the combustion of biogas[3] and offers the advantage of directly and very efficiently harnessing renewable electricity for chemical processes [24,25]; such electrical heated reforming reactors have already been successfully demonstrated [26,27].
- TriRef. The tri-reforming process is a variation of the bi-reforming process, whereby pure $O_2$ is fed into the reforming reaction chamber to provide the required heat through concurrently occurring exothermic oxidation. This approach eliminates the need for external energy input or removal (autothermal operation). Autothermal reforming is already commercially employed in the production of syngas from methane [28,29]. Within the TriRef configuration, sufficient $O_2$ is available from water-electrolysis.

The process flowsheet depicted in Fig. 3–1 applies to both configurations. Biogas is first purified in an adsorber bed filled with doped activated carbon without pressure or temperature adjustments.[4] Then, the cleaned biogas is compressed and mixed with steam (bi-reforming) or steam and oxygen (tri-reforming), depending on the respective process configuration; the reactant composition can be described with the ratio given by Eq. 3–1. Afterwards, the gas mixture is pre-heated and fed to the reforming reactor. The reformer product is then cooled down to condense the contained water. The remaining gas mixture (raw syngas) is compressed, mixed with light gases from the purification process (predominantly $CO_2$), and conditioned with pure hydrogen. The hydrogen can be supplied directly from the electrolyzer or the intermediate hydrogen storage tank. The stoichiometric number (*SN*, Eq. 3–2) and the carbon oxide ratio (*COR*, Eq. 3–3) characterize the syngas composition according to its molar composition.

$$OxyN = \frac{[CO_2] + [H_2O]}{[CH_4]} \tag{3–1}$$

$$SN = \frac{[H_2] - [CO_2]}{[CO] + [CO_2]} \tag{3–2}$$

$$COR = \frac{[CO_2]}{[CO] + [CO_2]} \tag{3–3}$$

with [x] being the molar fraction of the respective component (x).

The conditioned syngas is pre-heated and fed to the methanol reactor in the synthesis and purification section. The reactor output is cooled down to condensate methanol and water, separated from the remaining gas stream. The remaining gas phase, consisting mainly of unreacted syngas components and inert gases, is recycled to the reactor. A proportion of the recycle gas is purged to avoid an uncontrolled accumulation of inert gases and light by-products. The methanol–water mixture contains small amounts of dissolved gases and heavier by-products and is purified in a two-stage column system. The first column (topping column) mainly separates light components via the column head. Afterwards, the second column (methanol column) separates water and heavier components via the column bottom, allowing pure methanol to be recovered as the head product.

### 3.2. Data and assumptions

Below, data and assumptions needed for the modeling and techno-economic assessment are outlined. The supplementary information provides further data and descriptions.

#### 3.2.1. Technical data

The main data used to model the technical processes are listed in Table 3–2. The $CH_4/CO_2$-ratio, the inert gas fraction (IGF), and the water content define the biogas composition. Since the composition of biogas can vary significantly, the inert gas fraction and the $CH_4/CO_2$-ratio are considered in the parameter variation. Electrolysis is assumed stoichiometrically, with electrical and thermal flows derived from the assumed electrical efficiency of the electrolyzer. Due to the high operating temperatures of the reforming processes, equilibrium composition is assumed at the reactor outlets. The oxidation number is set to 1.5 (Eq. 3–1) to ensure an excess of oxidants and to prevent coking. The influence of the reforming temperature is analyzed within parameter variation. Syngas conditioning is controlled via design specifications, adjusting the stochiometric number (*SN*, Eq. 3–2) at the reactor entry to 2.05 and the inert gas fraction of the syngas to 20 %. The latter is also considered within parameter variation.

The methanol synthesis is modeled with a temperature approach considering the three main reactions; i.e., the conversion rate depends on the chemical equilibrium, whereby the respective temperature difference gives the offset from the equilibrium. The formation of by-products correlates linearly with the amount of methanol produced. Downstream separation is designed to enable methanol purity according to the quality of methanol grade AA.

#### 3.2.2. Economic data

In addition to technical parameters directly influencing the relative mass and energy balances, other technical parameters predominantly affect economic figures and do not change technical results. Furthermore, various economic assumptions can significantly impact economic key figures. The respective values and framework assumptions are listed in Table 3–3. The costs are given in euro currency and adjusted according to the chemical plant cost index (CEPCI) for 2022.

**Technical parameter.** The installed nominal capacity of the PBGtM plant is, from a technical perspective, limited by the availability of biogas at the plant site. The nominal capacity of the production facility typically does not affect the carbon and energy efficiency.[5] Still, it does influence the specific plant costs (economy-of-scale) and, consequently, the methanol production costs (*MPCs*). In the reference case, the plant size is designed for an available biogas quantity of 670 $Nm^3/h$, corresponding to a medium- to large-scale biogas plant. The influence of the plant size on the production costs is analyzed as part of economic parameter variation, where the plant size is varied using a scale factor concerning the reference case (scale factor 1). The annual plant's full load hours (*AFLH*) determine the annual production quantity at a given plant capacity, thus impacting the production costs. The annual full load hours are dependent not only on market-related factors but also on the technical availability of the biogas plant and the PBGtM plant itself. In the reference case, ca. 7,500 h/a (full load) are assumed (plant utilization of 85 %), constrained by the typical annual full load hours of biogas

[3] In-house simulations have shown carbon losses of about 25% when biogas is used for heating.

[4] Since the activated carbon filter has no relevant influence on the mass and energy flows of the overall process, it is not included in the modeling.

[5] Assuming the process concept, including process integration, remains unchanged, and the equipment is adapted to the respective performance classes. In very small-scale plants, the influence of heat losses can lead to reduced efficiencies.

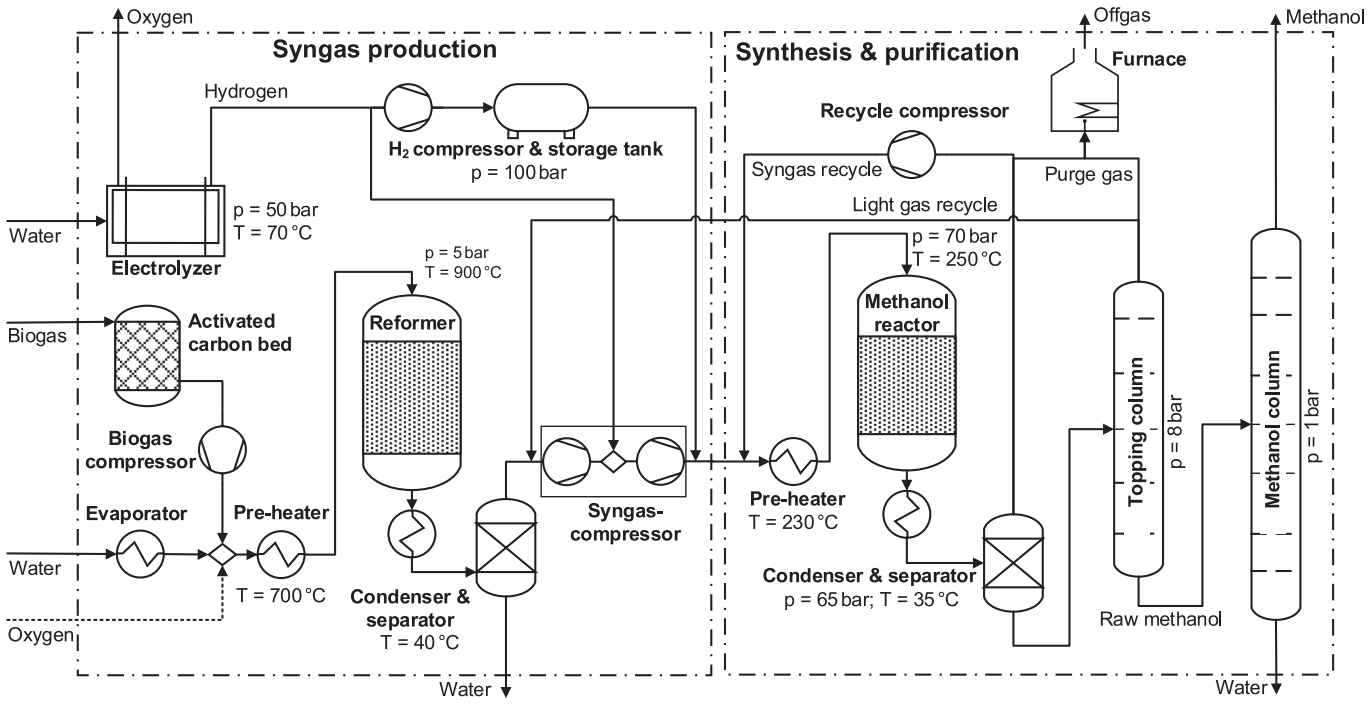


**Fig. 3–1.** PBGtM process flowsheet with main operating conditions. (Dotted line only in case of tri-reforming).

**Table 3–2**
Technical modeling data. (LHV: Lower heating value, PV: Parameter variation, RC: Reference case).

| Stream/ Process | Parameter | | Value | Reference |
|---|---|---|---|---|
| Biogas | Composition | $CH_4/CO_2$-ratio | RC: 1.5 \| PV:1 – 3 | [30–32] |
| | | $N_2$ [vol-%$_{Dry}$] | RC: 2 \| PV 0 – 5 | [30,31] |
| | | Dew point [°C] | 10 | [30] |
| Electrolysis | Conversion | $H_2O \rightarrow H_2 + 0.5\ O_2$ | 1 | [-] |
| | Energy demand | Electrical efficiency [%$_{LHV,\ H2}$] | 67 | [33] |
| Reforming | Operating conditions | *T* [°C] | RC: 900 \| PV: 800 – 1,000 | [32,34] |
| | | *p* [bar] | 5 | [34] |
| | Condition | *OxyN* (Eq. 3–1 | 1.5 | [34] |
| | Equilibrium conversion | Products considered: CO, $CO_2$, $H_2O$, $H_2$, $CH_4$, $O_2$, $N_2$ | | [23,35] |
| Methanol synthesis | Operating conditions | *T* [°C] | 250 | |
| | | *p* \| Δ*p* [bar] | 75 \| −5 | [5,36] |
| | | Inert gas share | RC: 0.20 \| PV: 0.02 – 0.50 | [-] |
| | Equilibrium conversion with temperature approach [K] | $CO + 2\ H_2 \leftrightharpoons CH_3OH$ | 15 | [37] |
| | | $CO_2 + 3\ H_2 \leftrightharpoons CH_3OH + H_2O$ | 15 | [37] |
| | | $CO + H_2O \leftrightharpoons CO_2 + H_2$ | 15 | [37] |
| Methanol | Share in final product | $CH_3OH$ [w-%] | 99.85 | [4] |

plants [38].

**Economic parameter.** The fixed capital investment (*FCI*) depreciation period is assumed to align with the plant's operating life. Uncertainties associated with estimating plant costs are assessed through the variation of annual capital costs (*ACC*) within the expected uncertainty range. The specific costs for biogas are determined based on the literature. Biogas production costs vary significantly depending on the utilized substrate and the plant capacity. The value provided in the reference case is at the lower end of the range, with higher values arising, especially for small-scale plants and potentially more complex substrates (e.g., straw). The biogas costs are currently predominantly assessed based on the energy content [€$_{2022}$/MWh$_{LHV}$], with no value attributed to the contained $CO_2$. The costs for continuously available electricity are estimated based on the European average price (2008–2020) for non-household electricity contracts. This value is in the same cost range as constant electricity supply costs from renewable power in the EU derived by [39]. Hydrogen supply costs are determined using an optimization model [20] by considering the 3rd. Quartile of the German onsite hydrogen supply cost for 2022 (see supplementary section 4 for extended results).

**Table 3–3**
Economic data and assumptions. (*ACC*: Annual capital cost, *AFLH*: Annual full load hours, PV: Parameter variation, RC: Reference case, SI: Supplementary information, WACC: Weighted average cost of capital).

| Process | Parameter | | Value | Reference |
|---|---|---|---|---|
| Plant related | Biogas capacity \| Scale factor | [Nm$^3$/h] \| [-] | RC: 670 \| PV: 0.1–100 | [-] |
| | *AFLH* | [h/a] | RC: 7,500 \| PV: 6,500–8,760 | [38] |
| Capital related | *WACC* (*i*) | [%] | RC: 6 \| PV: 0–12 | [20] |
| | Depreciation period (*n*) | [a] | 20 | [40,41] |
| | *ACC* uncertainty (Factor) | [-] | 0.7–1.5 | [22] |
| Costs | Biogas | [€$_{2022}$/MWh$_{LHV}$] | RC: 72 \| PV: 45–185 | [42,43] |
| | Electricity | [€$_{2022}$/MWh] | RC: 13 \| PV: 9–23 | [39,44] |
| | Hydrogen | [€$_{2022}$/kg] | RC: 7.0 \| PV: 5.0–9.0 | SI section 4 |

## 4. Technical results

Firstly, the process configurations are analyzed regarding the occurring carbon and energy flows in the reference case. Secondly, the influence of selected parameters on the technical key figures is shown. Lastly, the results are assessed and compared to non-hybrid production concepts regarding carbon utilization.

### 4.1. Process flow analysis

The process simulation results are used to visualize and evaluate the process configurations' relative carbon and energy flows under the reference case assumptions.

#### 4.1.1. Carbon flows

The carbon flows are depicted relative to the overall carbon input stream. Stoichiometrically, the carbon input can be bound entirely within the methanol product (carbon efficiency of 100 %) since the formation reactions do not include carbon-containing by-products. However, since conversions and separation processes are usually non-ideal, accumulations and losses occur, which are visualized in the flow diagrams. Hydrogen production is not depicted in the visualization since no carbon is involved.

**BiRef.** Fig. 4–1 shows the carbon flows of the BiRef configuration. Here, biogas is the only carbon-containing input. No relevant carbon losses occur during biogas conversion into syngas within bi-reforming and conditioning. However, as methane is not fully converted in the reforming process, methane is carried into the methanol synthesis as an inert gas in addition to nitrogen. Due to the equilibrium-limited syngas conversion in the methanol synthesis, which requires significant syngas recycling, carbon accumulation occurs within the synthesis loop. Here, carbon losses occur through purge gas release, which is required to avoid excessive inert gas accumulation. Methane represents more than 55 % of the inert components within the purge gas, resulting in purge-related carbon losses of 6 %.

The liquid synthesis product still includes 99 % of the utilized carbon when it's fed into the topping column. After separating dissolved gases (mainly $CO_2$), the raw methanol contains 93 % of the overall carbon input. Within the methanol column, methanol is sharply separated through multistage rectification; no further carbon losses occur at this stage.

The resulting overall carbon efficiency is 93 %, with the remaining carbon (7 %) released as flue gas. The assumed biogas input of 670 $Nm^3$/h enables a methanol production of 860 kg/h. The specific biogas demand is, therefore, 0.78 $Nm^3_{BG}/kg_{MeOH}$.

**TriRef.** Fig. 4–2 shows the carbon flows of the TriRef configuration. As in the BiRef configuration, no carbon losses occur during biogas conversion to syngas. However, gas composition at the reformer outlet differs significantly due to the additional oxygen injection into the autothermal reformer (Table 4–1). The higher carbon oxide ratio (Eq. 3–3) results in a lower per-pass conversion within the methanol reactor. Nevertheless, the carbon flow of syngas recycling is only slightly higher as in the BiRef configuration due to the significantly lower methane share of the inert gases (<15 %). Considering also carbon-free components, the volume flow of syngas in the TriRef configuration is 40 % higher than in the BiRef configuration. Since less inert gas is present in the fresh syngas, the carbon losses related to purge gas only account for 3 % of the utilized carbon, leading to an overall carbon efficiency of 97 % (i.e., 4 %pt. more than the BiRef configuration). In the reference case, a 900 kg/h methanol production capacity is reached based on a 670 $Nm^3$/h biogas feed, corresponding to a specific biogas demand of 0.74 $Nm^3_{BG}/kg_{MeOH}$.

#### 4.1.2. Energy flows

The process energy flows are normalized to the total energy input of the overall process to analyze and assess the major energy demands and losses of the process configurations. Thereby, chemical energy (related to the higher heating value; HHV), electrical energy, and thermal energy (heating and cooling demands) are considered. The supplementary information lists further information regarding heat integration.

**BiRef.** The energy flows of the BiRef configuration are depicted in Fig. 4–3, indicating that the main energy input takes place through biogas (59 %). The remaining energy is provided by electricity needed for $H_2$ production (25 %), heating requirements (12 %), and gas compression (4 %). Heating requirements (in the form of electrical power) are needed within the bi-reforming reactor since only a small part of the required heat can be integrated from internal heat sources (supplementary information, section 4.1). Internal heat sources like

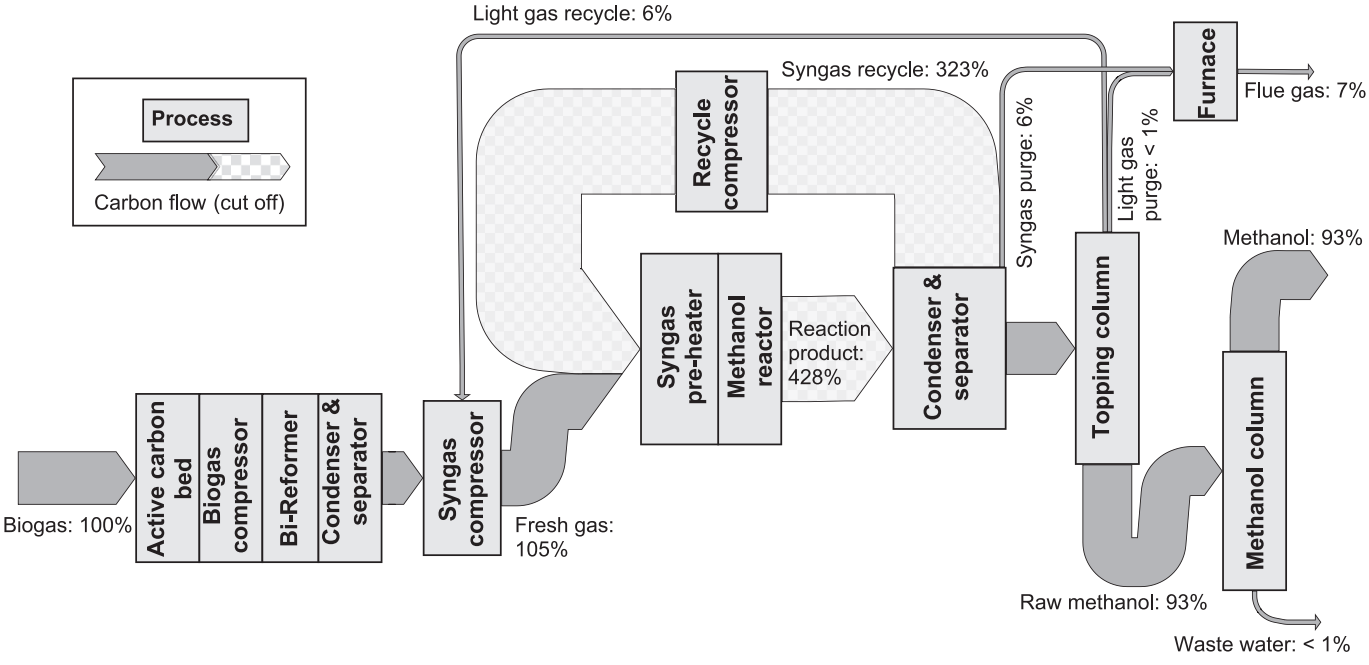


**Fig. 4–1.** Relative carbon flows of the bi-reforming configuration (BiRef).

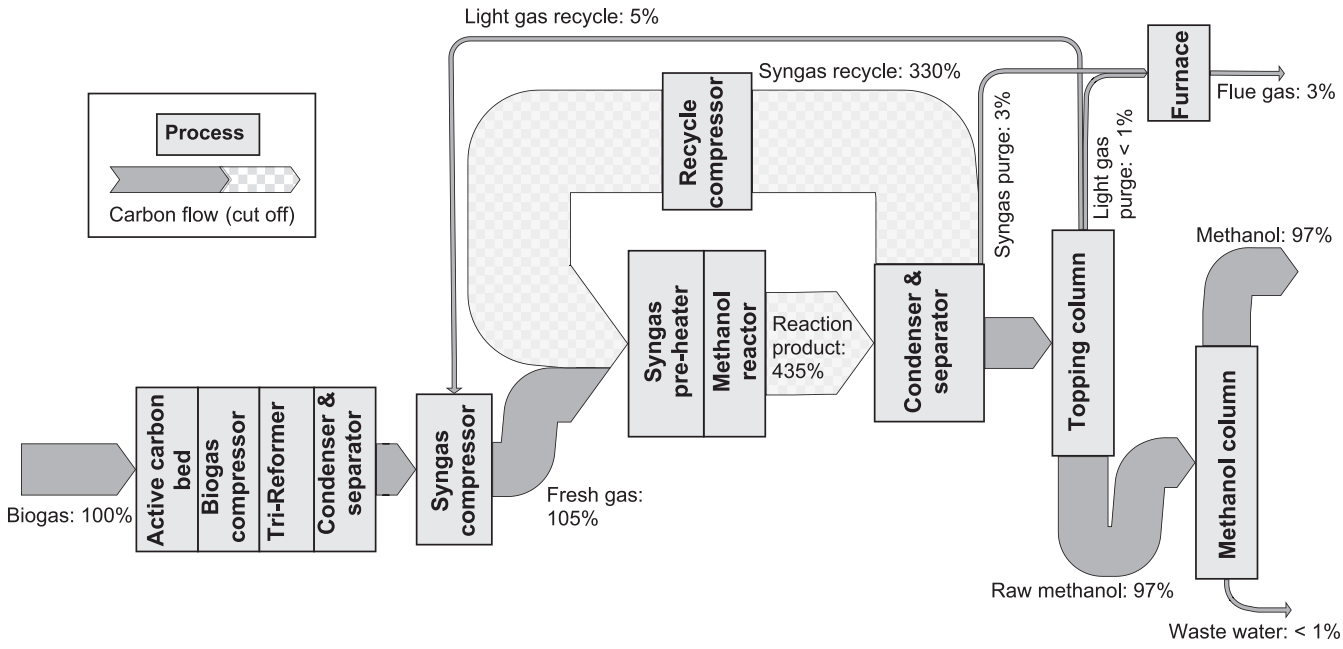


**Fig. 4–2.** Relative carbon flows of the tri-reforming configuration (TriRef).

**Table 4–1**
Gas properties of both process configurations. (*COR*: Carbon oxide ratio, *SN*: Stoichiometric number, IGF: Inert gas fraction).

| Parameter | BiRef configuration | | TriRef configuration | |
|---|---|---|---|---|
| | Reformer product | Reactor feed | Reformer product | Reactor feed |
| *SN* (Eq. 3–2) | 1.36 | 2.05 | 0.75 | 2.05 |
| *COR* (Eq. 3–3) | 0.11 | 0.42 | 0.32 | 0.62 |
| IGF [%] | 2 | 20 | 1 | 20 |

methanol synthesis can satisfy other internal heat demands. The overall energy efficiency is 74 %, while the remaining energy is released as waste heat, i.e., mainly via cooling water. The electricity demand of the electrolyzer under steady-state conditions is 1.8 $MW_{el}$, enabling a methanol output of 5.5 $MW_{HHV}$.

**TriRef.** Fig. 4–4 shows the energy flows of the TriRef configuration. Here, biogas represents 52 % of the overall energy input. Like in the BiRef configuration, electrical energy provides the remaining energy. However, in the TriRef configuration, the energy required for $H_2$ production is almost twice as high (3.6 $MW_{el}$) as in the BiRef configuration. This increase is due to the lower stoichiometric number of the reforming product (Table 4–1), caused by the additional $O_2$ input and the associated higher $CO_2$ and $H_2O$ formation. However, due to the autothermal reforming, no external heating demands exist, which partially compensates for the higher energy requirement of the electrolysis. Despite significantly larger amounts of $H_2$, the recycling loop's energy stream is lower than the respective stream in the BiRef configuration, as the methane contained in the BiRef configuration overcompensates for this. The overall energy efficiency results in 69 % (compared to 74 % for the BiRef configuration), while the remaining energy is released into the environment as low-temperature waste heat. The methanol production capacity in the reference case is about 5.7 $MW_{HHV}$.

### 4.2. Parameter variation

This section analyzes and compares the effects of changing parameters on the technical key figures of the overall process configurations. On the one hand, this results in quantitative findings on the impact of biogas-specific properties. On the other hand, technically advantageous operating ranges and associated optimization potentials can be identified.

The analysis of the reference cases shows that the TriRef configuration has a higher carbon efficiency than the BiRef configuration at the expense of a lower energy efficiency. Therefore, parameter variation is first analyzed in terms of carbon efficiency (Fig. 4–5 and Fig. 4–6, left), and following regarding energy efficiency (Fig. 4–5 and Fig. 4–6, right).[6]

#### 4.2.1. Carbon efficiency

Fig. 4–5 (left) shows the impact of different biogas compositions on the carbon efficiencies of the investigated process configurations. In the reference case, the inert gas fraction (IGF) (solid lines) is assumed to be 0.02, and the $CH_4/CO_2$-ratio (dashed lines) is 1.5.

- **Biogas – Inert gas fraction.** An increasing inert gas fraction of the utilized biogas negatively affects the carbon efficiencies for both process configurations. The BiRef configuration's carbon efficiency decreases almost linearly within the varied area from 94.6 to 90.7 %. The carbon efficiency of the TriRef configuration responds slightly stronger to an increasing inert gas fraction and decreases from 98.8 to 94.5 %.

In both configurations, the carbon losses are caused by increasing amounts of purge gas, which is only used energetically. The slightly lower sensitivity in the BiRef configuration is due to the anyway higher amount of inert gas present through unreacted methane.

- **Biogas ratio – $CH_4/CO_2$.** Since a linear variation of the $CH_4/CO_2$-ratio leads to a non-linear change in the respective $CH_4$ and $CO_2$ fraction, these variations also affect the carbon efficiency non-linear. An increasing ratio thereby decreases the carbon efficiency. Concerning the BiRef configuration, carbon efficiency decreases from 94.1 to 91.8 % in the varied area. The TriRef configuration shows

[6] Lines that do not cover the entire parameter variation range result from physical limitations of the modeled processes, where within the specified parameter ranges, the given design specifications can no longer be met, and therefore, no solutions exist for these parameters.

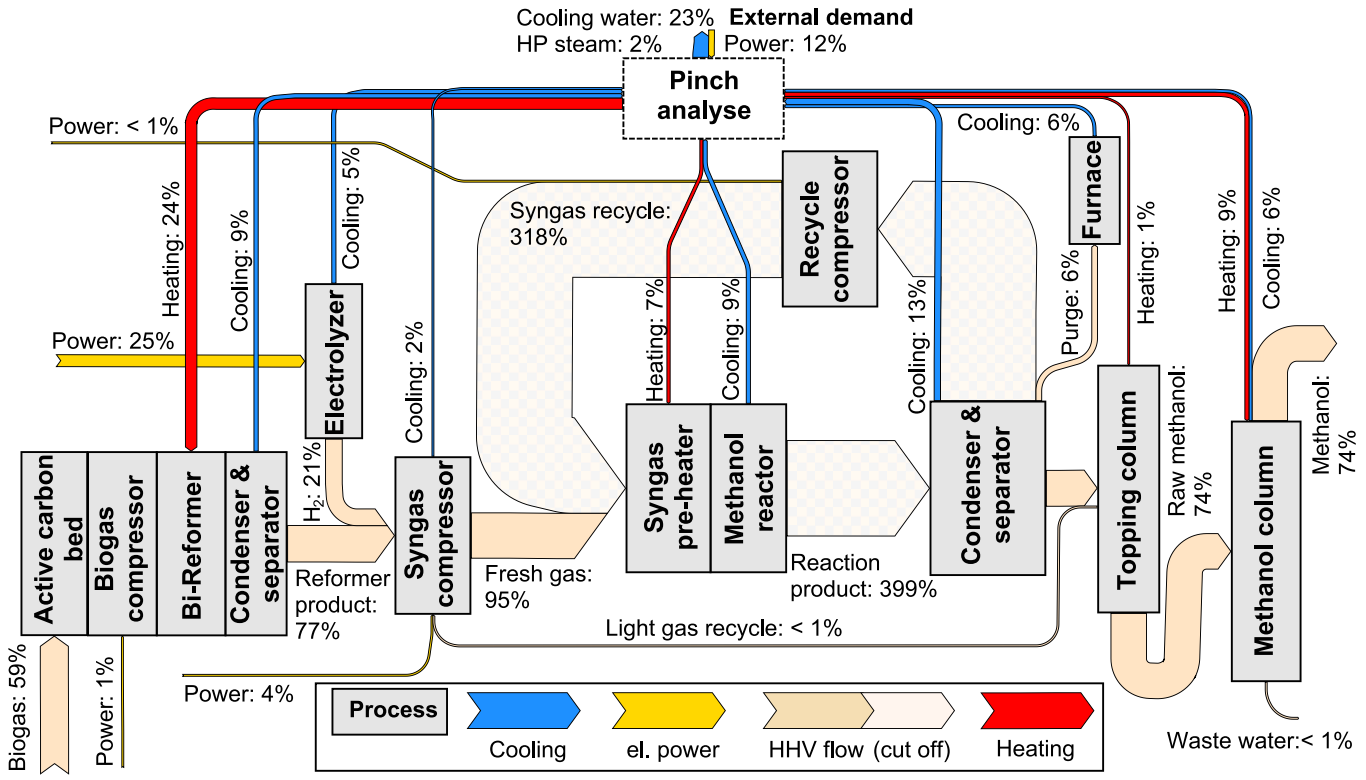


**Fig. 4–3.** Energy flows (rounded) of the biogas bi-reforming (BiRef) configuration. (Heating and cooling below 1% not depicted; el.: electrical, HHV: Higher heating value).

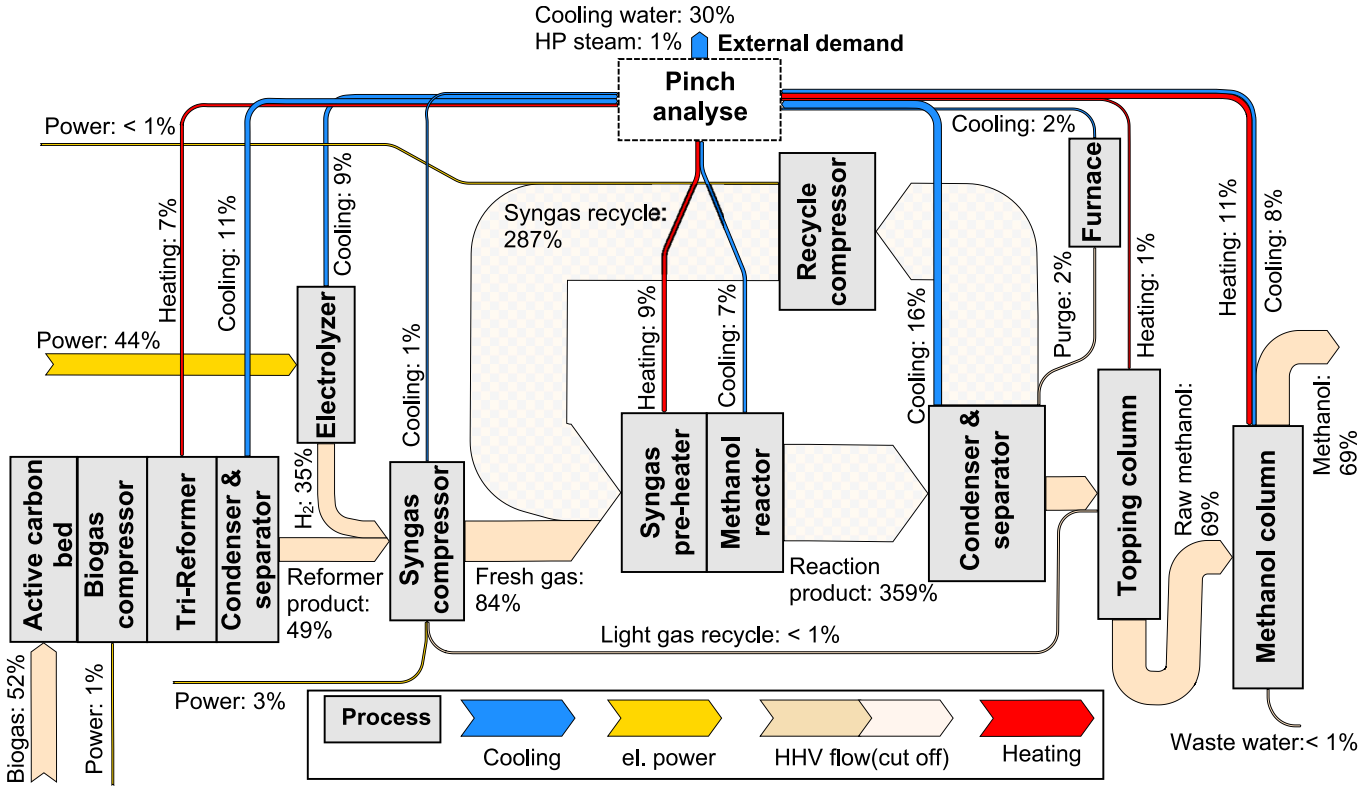


**Fig. 4–4.** Energy flows (rounded) of the biogas tri-reforming (TriRef) configuration. (Heating and cooling below 1% not depicted; el.: electrical, HHV: Higher heating value).

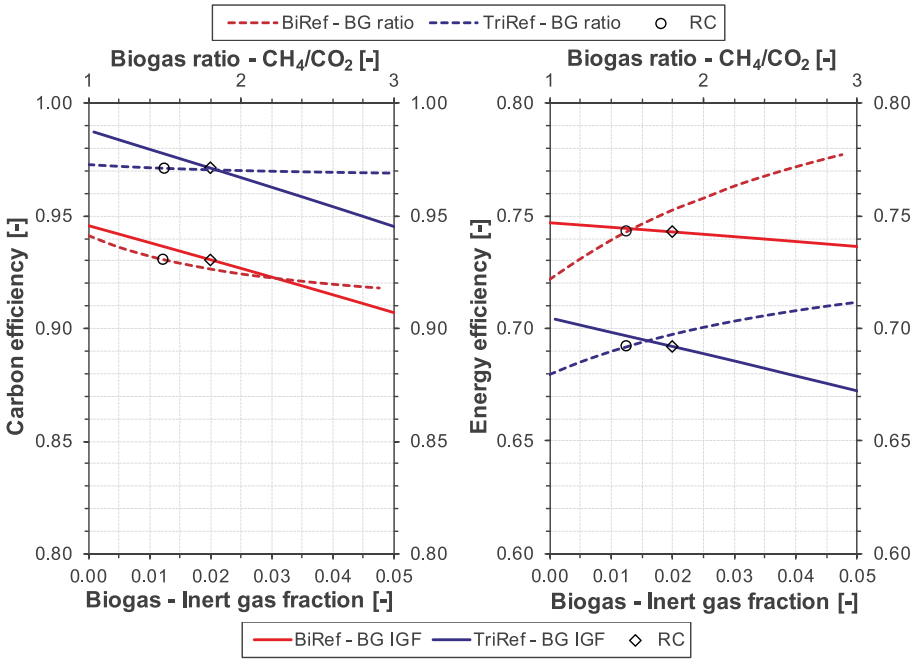


**Fig. 4–5.** Carbon (left) and energy (right) efficiency under variation of biogas inert gas fraction and biogas ratio. (BG: Biogas, BiRef: Process configuration with electrically heated bi-reforming, IGF: Inert gas fraction, RC: Reference case, TriRef: Process configuration with autothermal tri-reforming).

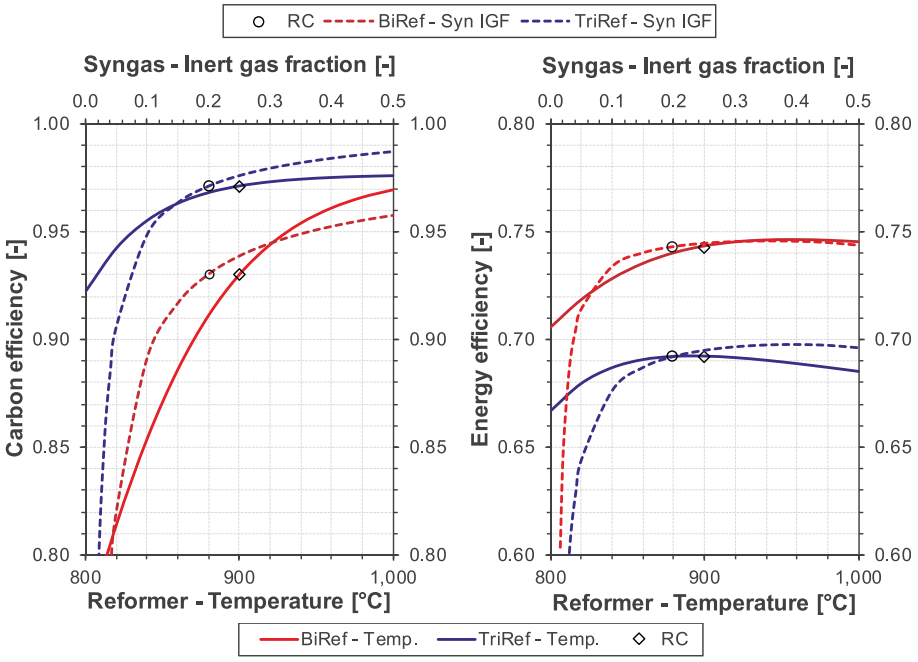


**Fig. 4–6.** Carbon (left) and energy (right) efficiency under variation of reformer temperature and inert gas fraction in syngas. (BiRef: Process configuration with electrically heated bi-reforming, RC: Reference case, Temp: Temperature, TriRef: Process configuration with autothermal tri-reforming, Syn: Syngas).

almost no response to the parameter variation and decreases only minimally from 97.3 to 96.9 %.

Since an increasing $CH_4/CO_2$-ratio implies an increasing $CH_4$ content, $CH_4$ conversion becomes more important with an increasing ratio. As the $CH_4$ content increases, the amount of unconverted methane in the reformer product also increases, which leads to higher purge gas amounts. Since lower conversions are achieved in the BiRef configuration, the effect is stronger than in the TriRef configuration.

Fig. 4–6 (left) shows the impact of changing process parameters on the carbon efficiencies of the investigated process configurations. In the reference case, the reformer temperature is set to 900 °C (solid lines), and the inert gas share in the reactor feed (dashed lines) is adjusted to 0.2.

- **Reformer – Temperature.** An increasing reformer temperature leads to a strongly non-linear increase in carbon efficiency. Especially in the lower temperature region analyzed, a rapid decrease of the key figure occurs. The carbon efficiency of the BiRef concept decreases sharply with reformer temperatures below 900 °C (93.0 to

76.8 %). Above 900 °C, the impact of increasing temperature decreases while carbon efficiency continues to grow (93.0 to 97.0 %). The curve of the TriRef configuration is similar but not quite as steep, and the shallow run-out begins at lower temperatures of about 820 °C. Carbon efficiency increases from 92.2 % to 97.6 % in the varied range.

The reforming temperature decisively determines the chemical equilibrium of the reforming reactions. Since high temperatures shift the equilibrium towards syngas formation, $CH_4$ conversion increases with increasing temperature, meaning less $CH_4$ enters the synthesis loop, and thus, less purge gas has to be purged. The significantly stronger influence on the BiRef configuration results from the lower oxidant amount compared to the TriRef configuration. Here, in addition to water and $CO_2$, $O_2$ is present as a very active oxidant, resulting in higher methane conversions even at lower temperatures.

- **Syngas – Inert gas fraction.** The inert gas fraction in the reactor feed results from the inert gas contained in the fresh gas concentrating with increasing recycling of unreacted syngas. The removal of purge gas controls the inert gas fraction (IGF). Thus, the curves resulting from the variation of the permitted inert gas fraction show an increase in carbon efficiency with increasing inert gas fraction. The curves are divided into an almost vertical part (IGF $< 0.1$) and a more horizontal part (IGF $> 0.2$). Starting from the reference case fraction (IFG $= 0.2$), the carbon efficiency drops steeply with decreasing permitted inert gas fraction. In both configurations, the carbon efficiency trends against the per-pass conversion when the inert gas fraction approaches the fresh gas inert gas fraction. In the area right of the reference case value, the carbon efficiency of the BiRef configuration increases up to 95.8 %. In the TriRef configuration, carbon efficiency increases up to 98.7 %.

In both configurations, the losses once again stem from purge gas. With increasing inert gas fraction in the synthesis loop, more inert components and fewer reactants are purged out within the same amount of purge gas. Again, the higher conversion enabled by tri-reforming shows advantages in the investigated area.

#### 4.2.2. Energy efficiency

Biogas properties and process parameters positively affecting carbon efficiency can lead to higher energetic efforts, which can exceed the energy benefit of higher production outputs. Below, the influence of parameter variation on energy efficiency is therefore analyzed in more detail. Fig. 4–5 (right) shows the impact of different biogas compositions on energy efficiency.

- **Biogas – Inert gas fraction.** The energy efficiency under variation of the biogas inert gas fraction (solid lines) shows a similar, almost linear trend as the carbon efficiency in the analyzed range. In both configurations, efficiency decreases with an increasing inert gas fraction. However, regarding the BiRef configuration, the slope is clearly lower compared to the carbon efficiency analysis. The energy efficiency decreases only slightly from 74.7 to 73.7 %. The TriRef configurations' energy efficiency responds stronger to an increasing biogas inert gas fraction, similar to the carbon efficiency, decreasing from 70.4 to 67.2 %.

The changes in energy efficiency result mainly from changes in methanol production (carbon efficiency). However, in the BiRef configuration, the increasing purge gas also increases the high-temperature heat utilized for bi-reforming. This additional heat reduces the electrical power demand and partly counteracts energy losses. Autothermal tri-reforming demands no external heating. Therefore, the heat of purge gas combustion can only be used if external heat sinks are available at the production site, which is not assumed within the analyzed configurations.

- **Biogas ratio – $CH_4/CO_2$.** The variation of the biogas ratio (dashed lines) shows that high ratios positively affect the energy efficiency of the configurations. Despite decreasing carbon efficiency, energy efficiency significantly increases in both configurations. In the case of the BiRef configuration, the energy efficiency rises from 72.2 to 77.7 %. The increase for the TriRef configuration is slightly lower, increasing from 68.0 to 71.1 %.

The variations in energy efficiency are primarily driven by the decreasing $H_2$ demand with increasing $CH_4$ content in the biogas, reducing the amount of electrical energy for the electrolysis. In comparison to biogas-based $H_2$ production (via reforming), this process is associated with higher losses. However, the additional $O_2$ input in tri-reforming requires additional $H_2$, even at high $CH_4/CO_2$ ratios. For the BiRef configuration, the external $H_2$ demand approaches zero for ratios close to three.

The influences of the process parameters reforming temperature (solid lines) and syngas inert gas fraction (dashed lines) on the overall energy efficiencies for both configurations are depicted in Fig. 4–6 (right).

- **Reformer – Temperature.** The energy efficiency of both process configurations exhibits an initially increasing trend as the reforming temperature increases, followed by a slight decrease after reaching a maximum. In the case of the BiRef configuration, the maximum is located at 960 °C and reaches 74.6 %. With a further temperature increase to 1,000 °C, the efficiency decreases slightly by 0.1 %. For the TriRef configuration, the maximum is reached at 900 °C with 69.2 %. Subsequently, the efficiency decreases by up to 0.7 % at 1,000 °C. In the range left of the maximum, the efficiencies of the BiRef and TriRef configuration drop to 70.5 and 66.7 %, respectively.

From a process level perspective, the trend in both curves results from, on the one hand, the increasing methanol yield (carbon efficiency) with rising reforming temperature and, on the other hand, the counteracting increase in energy demand for reforming. As the positive impact of higher reforming temperatures on the methanol output decreases, particularly in the TriRef configuration, the increasing energy demand predominates, leading to a decrease in energy efficiency beyond the maximum.

In the case of bi-reforming, the additional energy demand is provided through electrical heating with an efficiency of 100 %. In the case of tri-reforming, the increase in temperature is achieved by increasing the oxygen input, which in turn raises the $H_2$ demand. However, $H_2$ production involves losses due to the electrolyzer efficiency of approximately 79 $\%_{HHV}$.

- **Syngas – Inert gas fraction.** The trend of the energy efficiency curves fundamentally exhibits similarities to those of carbon efficiency. However, the curves attain a maximum within high inert gas fractions before falling slightly again. In the varied area of permitted syngas inert gas fractions, the BiRef configurations' energy efficiency increases from 64.9 % at 2 $\%_{IGF}$ to 74.6 % at 35 $\%_{IGF}$, which decreases then to 74.4 % at 50 $\%_{IGF}$. The TriRef configurations' energy efficiency increases from 55.3 % at 2 $\%_{IGF}$ to 69.7 % at 40 $\%_{IGF}$. The efficiency then decreases slightly to 69.6 % at 50 $\%_{IGF}$.

In both configurations, efficiency gains driven by increasing methanol production predominate up to the maximum. Furthermore, due to the slightly over-stoichiometrically operated syngas, fresh gas $H_2$ demand and the associated electrolysis power decrease with increasing recirculation. However, beyond the maximum, the exponentially increasing quantity of recycling gas and the consequent electrical energy demand of the recycling compressor outweigh the benefits.

### 4.3. Assessment

The following summarizes and assesses the technical results (Fig. 4–7). The reference analysis (red and blue horizontal lines) shows differences in carbon and energy efficiency between the BiRef and the TriRef configuration. The advantage of the TriRef configuration in terms of carbon efficiency and the associated lower biogas demand result from the higher methane conversion in the reforming process caused by the addition of oxygen. However, this is accompanied by an increase in hydrogen demand. Since converting electricity into heat (bi-reformer) is more efficient than converting electricity into hydrogen (electrolysis), the BiRef configuration enables a higher energy efficiency despite the lower methanol output.

The composition of the biogas can vary significantly depending on the substrate used and the operating conditions of the biogas plant. The influences on the efficiency of the PBGtM concept determined in the parameter variation are assessed as moderate. A low $N_2$ content in the biogas is generally favorable and increases carbon and energy efficiency. A high methane content in the biogas reduces the electrolysis demand and thus increases the overall energy efficiency, while the carbon efficiency is mainly unaffected, especially when using tri-reforming.

In contrast to the given properties of biogas, process parameters can be directly influenced by process design and operation. Therefore, parameter variation results represent potentials for technical process optimization. The influence of the reformer temperature and the syngas inert gas fraction on the technical key figures is very strong; however, only limited improvements can be achieved compared to the reference case. Significant improvements can only be achieved in the BiRef configuration. Specifically, elevated reformer temperatures enable an increase in carbon efficiency up to the level of the TriRef configuration. An increase in the permissible inert gas fraction also increases carbon efficiency. However, regarding the energy efficiency, increasing process-related energy demands prevent enhancements from both process parameters.

Comparison with non-hybrid methanol production from biogas

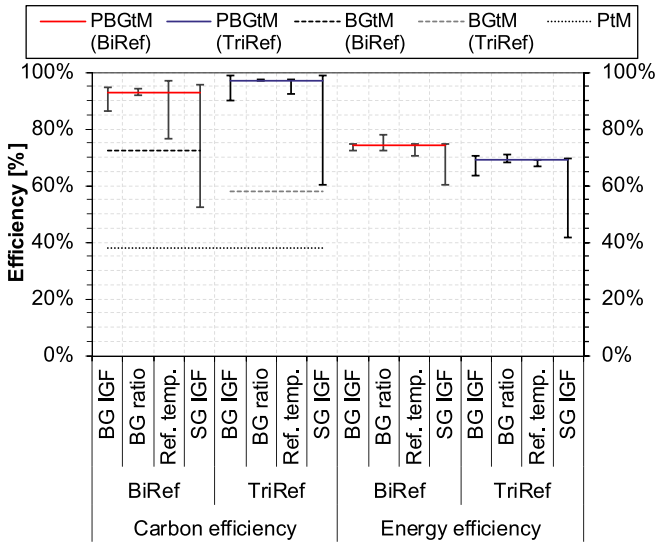


**Fig. 4–7.** Summary comparison of technical reference case and parameter variation results. (BG: biogas, BGtM: Biogas-to-Methanol, BiRef: Process configuration with electrically heated bi-reforming, IGF: Inert gas fraction, PtM: Power-to-Methanol, RC: Reference case, Ref. temp.: Reformer temperature, SG: Syngas, TriRef: Process configuration with autothermal tri-reforming).

(Fig. 4–7) reveals that integrating electricity-based hydrogen increases carbon efficiency substantially. For purely electricity-based production (PtM), utilizing only the $CO_2$ share of the biogas, carbon efficiency decreases to only 38 %.[7] Purely biogas-based production (BGtM) achieves carbon efficiencies of 72.5 % with electrically heated bi-reforming and 58.2 % with tri-reforming. Since the carbon efficiency directly correlates with methanol production, non-hybrid concepts produce significantly lower quantities of methanol. For the biogas composition assumed within the reference case, an increase in methanol yield of 28 % (BiRef) and 67 % (TriRef) is achieved compared to the purely biogas-based concepts. The hybrid approach is particularly advantageous when the biogas has a high $CO_2$ content while the significance of adding electricity-based hydrogen diminishes as the $CH_4$ share increases. Considering a biogas ratio ($CH_4/CO_2$) of three within a bi-reforming-based configuration, carbon efficiency increases by only 2 %pt. through additional hydrogen input. However, considering tri-reforming, hydrogen addition still increases carbon efficiency by 24 %pt. In summary, the assessment shows that both PBGtM configurations significantly increase the targeted carbon utilization compared to non-hybrid concepts.

## 5. Economic results

First, the methanol production costs resulting from the reference case are discussed, followed by an analysis of various influencing parameters and the assessment compared to non-hybrid product concepts.

### 5.1. Production costs

Fig. 5–1 (left columns) illustrates the methanol production costs resulting from both process configurations in the reference case. The costs are compared with those of non-hybrid concepts (right columns) and fossil fuel-based production in section 5.3.

Estimating production costs for methanol in the BiRef configuration reveals a relatively even distribution of the various cost components. The largest share of costs is attributed to biogas supply. The second largest cost contribution is fixed operational expenditures, predominantly determined by various labor expenses and maintenance. Hydrogen costs are also substantial, while electricity and annual capital costs are slightly lower.

In the TriRef configuration, nearly identical methanol production costs result. Due to the absence of heating in the tri-reforming reactor, the TriRef configuration requires slightly lower fixed capital investments, leading to annual capital costs and parts of the fixed operational expenditures being lower than those in the BiRef configuration. Biogas costs are also slightly lower due to higher carbon efficiency. The largest cost component results from hydrogen supply, accounting for 42 % of the methanol production costs. Electricity costs are relatively low compared to the BiRef configuration due to the lower relative demand.

### 5.2. Parameter variation

The following analyzes the impacts of various technical and economic parameters on methanol production cost (*MPC*) by parameter variation. The investigation areas are defined to follow the technical results from parameter variation and typical market and project-related cost ranges.

#### 5.2.1. Technical parameters

In the context of the technical analysis, the parameter variation revealed different carbon and energy efficiencies for the investigated plant configurations. The influences of these efficiencies on the *MPCs* are depicted in Fig. 5–2.

For both configurations, the parameter variation shows only marginal cost reductions with improvements in efficiency compared to the reference case. Across the entire range of technical key figures, the *MPCs*

[7] Carbon capture rate of 95% assumed.

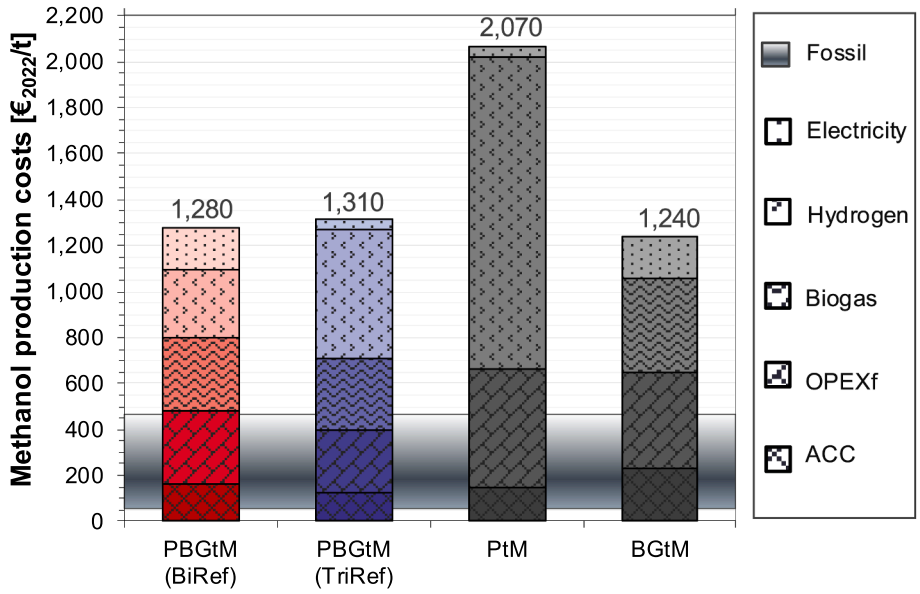


**Fig. 5–1.** Methanol production costs for the reference case. (Assumptions for PtM and BGtM see supplementary information, fossil cost range according to [6,45]; ACC: Annual capital cost, BGtM: Biogas-to-Methanol, PtM: Power-to-Methanol; OPEXf: Fixed operational expenditures).

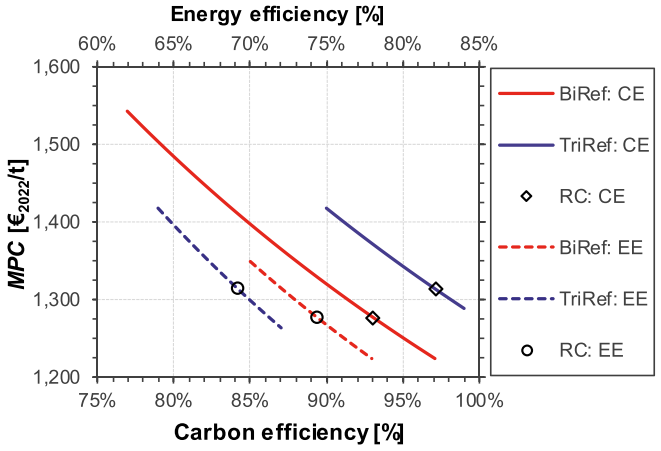


**Fig. 5–2.** Effect of carbon and energy efficiency variation on methanol production cost. (CE: Carbon efficiency, EE: Energy efficiency, *MPC*: Methanol production cost, RC: Reference case).

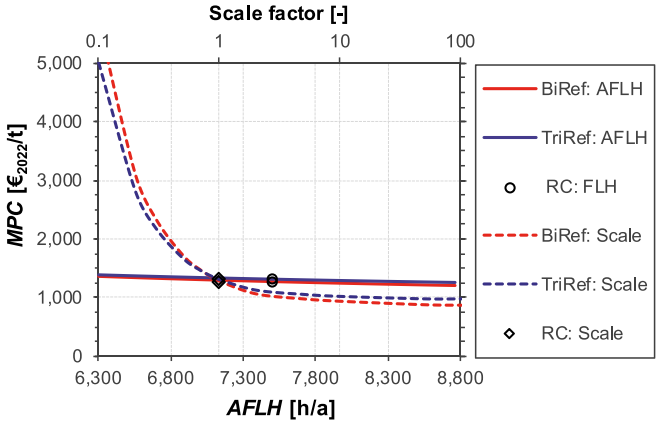


**Fig. 5–3.** Effect of AFLH and plant scale on methanol production cost. (Scale factor 1 corresponds to the reference case with 670 $Nm^3_{BG}/h$; *AFLH*: Annual full load hours, *MPC*: Methanol production cost, RC: Reference case).

fluctuate by around 150 $€_{2022}$/t. An exception to this is the variation in carbon efficiency in the case of the BiRef configuration. Here, insufficient reforming temperatures or very low permissible inert gas concentrations in the syngas can significantly increase costs due to reduced product formation. However, these losses can be avoided through suitable plant design and operation.

The impacts of annual full load hours (*AFLH*) and plant capacity (scale factor) on *MPCs* are illustrated in Fig. 5–3.

The variation of annual full load hours, which is varied around ± 16 % from the reference case (RC), results in an *MPC* variation of about 160 $€_{2022}$/t and 130 $€_{2022}$/t for the BiRef and TriRef configuration, respectively. Increasing annual full load hours from the reference case to a hypothetical annual full load (8,760 h/a) leads to cost reductions of around 5 % for both configurations.

The variation in plant capacity spans a wide scaling range (factor 1,000). Here, reducing the assumed reference case capacity has a stronger effect than increasing it. Doubling the capacity results in a relative *MPC* reduction of 17 % (BiRef) and 14 % (TriRef), while halving the capacity leads to an *MPC* increase of 34 % (BiRef) and 28 % (TriRef).

Sensitivity to changes in plant size is somewhat more pronounced for the BiRef configuration than for the TriRef configuration. Increasing capacity by a factor of 10 reduces *MPC* by approximately 27 % (BiRef) or 22 % (TriRef). However, decreasing capacities affect the *MPC* much more strongly.

### 5.2.2. *Economic parameters*

Fig. 5–4 shows the influence of annual capital cost (*ACC*) and weighted average capital cost (*WACC*) on *MPC*. The annual capital cost variation shows a linear trend with a higher gradient for the BiRef configuration. However, *MPCs* vary less than −50 $€_{2022}$/t and +100 $€_{2022}$/t from the reference case for both configurations. The weighted average capital costs have a non-linear impact on *MPC*. Higher fixed capital investments are more affected by changing weighted average capital costs. Therefore, the costs from the BiRef configuration change slightly more than in the TriRef configuration. However, the influence of the weighted average capital costs for the assumed variation areas is only marginally higher than the variation of the annual capital cost.

Fig. 5–5 depicts the influences of material and energy feedstock costs

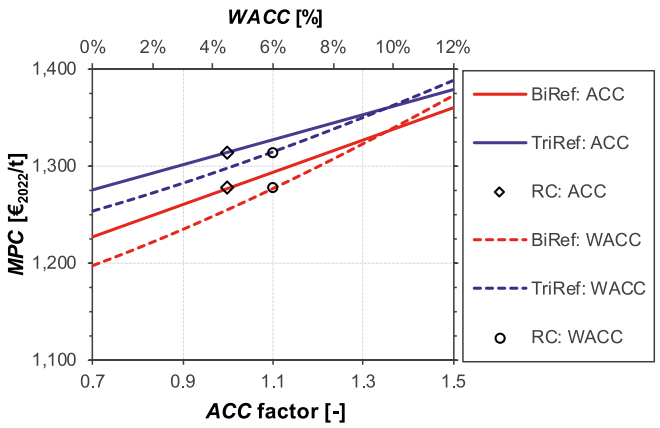


**Fig. 5–4.** Effect of *ACC* and *WACC* on methanol production cost. (*ACC*: Annual capital cost, *MPC*: Methanol production cost, RC: Reference case, *WACC*: Weighted average cost of capital).

on *MPC*. Due to the wide cost range of biogas (variation factor of 4), which can increase significantly from the reference case, especially for small-scale biogas plants and complex substrates, parameter variation can also lead to significant changes in *MPC*. A 50 % increase in the biogas costs results in an *MPC* increase of around 12 % in both configurations compared to the reference case. However, since biogas production costs can also vary to a much greater extent, the change in *MPC* from the reference case can range from −121 €$_{2022}$/t (10 %) to + 507 €$_{2022}$/t (40 %) in the case of the BiRef configuration and from −116 €$_{2022}$/t (9 %) to + 486 €$_{2022}$/t (37 %) in the case of the TriRef configuration.

The considered electricity costs vary by a factor of 2.6 across the entire range. A 50 % increase in electricity costs results in a 91 €$_{2022}$/t (7 %) cost increase in the BiRef configuration and 24 €$_{2022}$/t (2 %) in the TriRef configuration. Across the entire variation range, there is a cost change relative to the reference case ranging from −56 €$_{2022}$/t (4 %) to + 140 €$_{2022}$/t (11 %) in the case of the BiRef configuration and from −15 €$_{2022}$/t (1 %) to + 37 €$_{2022}$/t (3 %) in the case of the TriRef configuration. The BiRef configuration shows lower *MPC* until electricity costs reach 17 €$_{2022}$/MWh.

The costs of constant hydrogen supply vary by ca. ± 30 % across the optimization scenarios (supplementary information, section 4). Given the significantly higher hydrogen demand of the TriRef configuration, cost sensitivity is notably higher compared to the BiRef configuration.

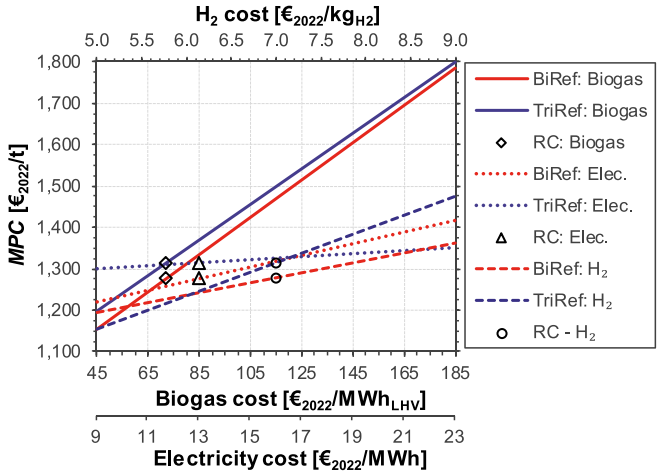


**Fig. 5–5.** Effect of biogas, electricity, and hydrogen cost on methanol production cost. (RC: Reference case, Elec: Electricity cost, *MPC*: Methanol production cost).

The fluctuations in the *MPC* amount to ± 84 €$_{2022}$/t (7 %) in the BiRef configuration and ± 159 €$_{2022}$/t (12 %) in the TriRef configuration. Cost advantages for the TriRef configuration are realized when hydrogen costs fall below 6 €$_{2022}$/kg$_{H2}$.

### 5.3. Assessment

The following summarizes and assesses the results of the economic analysis. The *MPCs* in the reference case are similar for both configurations, with the BiRef configuration leading to slightly lower costs primarily due to the lower hydrogen demand. Both PBGtM configurations exhibit a relatively even distribution of cost components. The main cost difference between the configurations lies in the proportions of hydrogen and electricity costs. Due to the significantly higher hydrogen demand, the associated costs are notably higher in the TriRef configuration. This cost difference is only partially offset by the higher electricity costs in the BiRef configuration. Besides the uncertainties inherently associated with calculating equipment costs, an increased uncertainty arises for the costs of the electrically heated reformer since the current literature does not provide the respective cost functions. However, considering the relatively low impact of the annual capital costs, significant deviations from the presented findings are not to be expected.

The parameter variation reveals that the ranges for expected efficiencies from the technical analysis have little impact on *MPCs*. The same applies to the impact of annual full load hours within the considered range. The installed plant capacity significantly impacts *MPCs*, particularly due to the broad variation range and strong economy-of-scale effects. Increasing the plant size leads to significant specific cost reductions compared to the reference case. Conversely, lower plant capacities have an even more pronounced effect; halving the capacity results in an *MPC* increase of around 30 %. Concerning the reference case, *MPC* reductions of over 20 % results for plants with tenfold capacity. However, only a few biogas plants worldwide have the necessary capacity to supply the needed amount of biogas for such a scale.

Changes in economic framework assumptions within the varied limits lead to minor *MPC* variations (<±10 % from the reference case). Significant *MPC* changes, on the other hand, can result from cost fluctuations of material and energy feedstocks. In particular, considering biogas production costs from the upper literature range can lead to an increase in the *MPC* of almost 40 %. The impact of hydrogen costs is especially relevant for the TriRef configuration. However, changes in the *MPCs* are below 12 %.

Compared to the literature, the determined costs of approximately 1,300 €$_{2022}$/t are above those reported for biomass-based methanol [6]. Compared to electricity-based methanol, the costs fall within the lower range of current estimations [6]. However, biogas as well as electricity-derived methanol, exhibit significant cost variations depending on the assumed process concept, feedstock, plant size, and economic parameters. Within the framework conditions applied here, PBGtM shows a clear cost advantage over purely electricity-based methanol (PtM) (Fig. 5–1). This advantage is due to the high costs of hydrogen supply and the significantly lower production capacity (assuming the same biogas potential). Purely biogas-based *MPCs* are in the same cost range as hybrid production. The advantage of BGtM lies in the absence of any additional hydrogen-related costs. However, lower product output disadvantageously offsets this due to higher specific fixed capital investments and fixed operational expenditures.

The *MPCs* of fossil fuel-based methanol from natural gas or coal range from 60 to 470 €$_{2022}$/t (without considering the costs of fossil $CO_2$ emission) [45], significantly lower than the achievable costs here. These low production costs for fossil-based methanol are achieved in countries with low natural gas or coal costs. The production facilities have capacities of up to 10,000 t/d, resulting in significantly reduced specific labor and maintenance costs compared to the decentralized PBGtM concept. Furthermore, the specific equipment costs are considerably

lower due to economy-of-scale effects. Given the global overcapacity for fossil-based methanol production, market prices are closely aligned with production costs. Assuming costs for $CO_2$ certificates of 81 €$_{2022}$/t [46] would lead to fossil *MPCs* increase of ca. 40 to 300 €$_{2022}$/t considering only process emissions according to [6,47,48]. Compared to conventional large-scale production plants, the PBGtM concept shows high fixed operational expenditures resulting mainly from high specific labor, maintenance, and plant costs.

Without an additional GHG-emission-related incentive compared to fossil fuel-based methanol, PBGtM-based methanol is not economically viable. The $CO_2$ mitigation costs are around 600 €$_{2022}$/t$_{CO2}$ for natural gas-based methanol and 250 €$_{2022}$/t$_{CO2}$ for hard coal-based methanol.[8] Economic advantages of the PBGtM concept over pure biogas- or electricity-based concepts primarily stem from downstream economy-of-scale benefits due to the higher utilization of feedstock (high carbon efficiency) and consequently larger methanol production capacities, as well as the cost-free supply of $CO_2$. Potential cost reduction for the concept lies in the standardized manufacturing of the plant as an end-of-pipe technology and in extensive automation for remote operation, as it is already common in biogas upgrading facilities.

## 6. Conclusion

The overall objective of the paper is to determine the efficiencies and costs of combined electricity- and biogas-based methanol production and to assess the concept compared to non-hybrid production approaches. Two process configurations based on different reforming technologies, i.e., BiRef configuration and TriRef configuration, were simulated and analyzed in a reference case and in a parameter variation. The key technical results can be concluded as follows:

- The BiRef configuration achieves a carbon efficiency of 93 %, while the TriRef configuration reaches 97 % (both for the reference case). Carbon efficiency advantages result from the higher methane conversion of tri-reforming, achieved through the additional use of oxygen as an oxidizing agent, allowing for lower purge gas quantities in the synthesis loop.
- The energy efficiency of the BiRef configuration reaches 74 %, while the TriRef configuration shows a lower efficiency of 69 % (both for the reference case and based on the higher heating value). The higher energy demand of the TriRef configuration primarily results from the higher hydrogen deficit of the reformer product, which must be compensated for by increased electrolysis capacity. In comparison, electrically heated bi-reforming utilizes electrical energy more efficiently.
- Changes in biogas composition only have a moderate effect on the efficiency of the configurations. A lower inert gas content in the biogas is advantageous for achieving higher carbon efficiencies. The demand for electricity-derived hydrogen decreases with an increasing $CH_4/CO_2$-ratio. The process parameters, reforming temperature, and syngas inert gas fraction significantly influence the investigated key figures. Generally, increasing these process parameters improves the carbon efficiencies of the configurations. However, the maximum energy efficiencies are not at the upper limit of the parameter range, as the increased energy demands surpass the elevated product formation.
- Compared to purely biogas-based methanol production (BGtM), the additional integration of electricity-based hydrogen can significantly increase carbon efficiency. For the reference case, efficiency enhancements of 21 %pt. (BiRef) and 39 %pt. (TriRef) are observed. Consequently, methanol yield can be increased by 28 % and 67 %, respectively. The significance of hydrogen addition is particularly important when employing tri-reforming and dealing with low methane content in biogas.

The results of the economic analysis can be concluded as follows:

- Under the assumed conditions applied in the reference case, the methanol production costs for both PBGtM configurations are around 1,300 €$_{2022}$/t, with minor advantages for the BiRef configuration. The hydrogen costs strongly drive the methanol production costs of the TriRef configuration. The cost shares of the BiRef configurations are more balanced, with biogas, hydrogen, and fixed operational expenditures being the main cost components.
- The methanol production costs are only slightly affected within the expected carbon and energy efficiency ranges. In contrast, plant capacity significantly affects production costs, showing cost reductions of over 20 % for plants with methanol production capacities exceeding 9 t/h, compared to 0.9 t/h in the reference case. While economic parameters show only minor effects on the methanol production costs, the availability of inexpensive biogas is essential, as high biogas costs can lead to cost increases of more than 37 %.
- Cost advantages compared to non-hybrid concepts (BGtM and PtM) arise from higher production capacities and the cost-free utilization of $CO_2$. However, the high costs associated with hydrogen supply result in methanol production costs at a similar level to those of purely biogas-based production. Due to the comparatively small production capacity and the more cost-intensive input materials, the production costs significantly exceed current fossil fuel-based methanol costs, resulting in $CO_2$ avoidance costs of between 250 €$_{2022}$/t$_{CO2}$ and 600 €$_{2022}$/t$_{CO2}$.

The investigated production concept offers the opportunity to make sustainable biomass resources available for material use and significantly increases carbon efficiency and production capacity compared to purely biogas-based concepts. However, challenges exist in the technical implementation of the complex production process in a decentralized, non-industrial setting and in the economic competitiveness with fossil fuel-based and purely biomass-based production concepts. However, the PBGtM concept can efficiently unlock additional carbon potentials, becoming increasingly important with the growing scarcity of available biomass and GHG-neutral carbon.

## CRediT authorship contribution statement

**Stefan Bube:** Writing – original draft, Software, Methodology, Investigation, Conceptualization. **Lucas Sens:** Writing – review & editing, Validation, Software. **Chris Drawer:** Writing – review & editing. **Martin Kaltschmitt:** Supervision, Conceptualization.

## Declaration of competing interest

The authors declare that they have no known competing financial interests or personal relationships that could have appeared to influence the work reported in this paper.

## Data availability

Data will be made available on request.

## Appendix A. Supplementary material

Supplementary data to this article can be found online at https://doi.org/10.1016/j.enconman.2024.118220.

[8] Assuming: GHG-neutral PBGtM production, fossil methanol combustion emissions of 1.375 t$_{CO2}$/t$_{Methanol}$, process emission of 0.5 t$_{CO2}$/t$_{Methanol}$ and 3.0 t$_{CO2}$/t$_{Methanol}$ for natural gas- and coal-based methanol production [6,47,48].

## References


[1] Umweltbundesamt. Atmosphärische Treibhausgas-Konzentrationen. [November 14, 2022]; Available from: https://www.umweltbundesamt.de/daten/klima/atmosphaerische-treibhausgas-konzentrationen#kohlendioxid-.

[2] Rodin V, Lindorfer J, Böhm H, Vieira L. Assessing the potential of carbon dioxide valorisation in Europe with focus on biogenic CO2. J CO2 Util 2020;41:101219. https://doi.org/10.1016/j.jcou.2020.101219.

[3] Fasihi M, Efimova O, Breyer C. Techno-economic assessment of CO2 direct air capture plants. J Clean Prod 2019;224:957–80. https://doi.org/10.1016/j.jclepro.2019.03.086.

[4] Ott J (ed.). Ullmann's Encyclopedia of Industrial Chemistry: Methanol. Weinheim, Germany: Wiley-VCH Verlag GmbH & Co. KGaA; 2012.

[5] Dieterich V, Buttler A, Hanel A, Spliethoff H, Fendt S. Power-to-liquid via synthesis of methanol, DME or Fischer–Tropsch-fuels: a review. Energy Environ Sci 2020;13(10):3207–52. https://doi.org/10.1039/D0EE01187H.

[6] International Renewable Energy Agency (IRENA) and the Methanol Institute. Innovation Outlook: Renewable Methanol. Abu Dhabi; 2021.

[7] IEA - International Energy Agency. The future of petrochemicals. OECD; 2018.

[8] Bertau M, Offermanns H, Plass L, Schmidt F, Wernicke H-J. Methanol: The Basic Chemical and Energy Feedstock of the Future. Berlin, Heidelberg: Springer Berlin Heidelberg; 2014.

[9] Entesari N, Goeppert A, Prakash GKS. Renewable methanol synthesis through single step bi-reforming of biogas. Ind Eng Chem Res 2020;59(22):10542–51. https://doi.org/10.1021/acs.iecr.0c00755.

[10] Acquarola C, Bhatelia T, Pareek V, Ao M, Shah MT. Optimized process for methanol production via bi-reforming syngas. Ind Eng Chem Res 2022;61(16):5557–67. https://doi.org/10.1021/acs.iecr.1c04904.

[11] Acquarola C, Ao M, Bhatelia T, Prakash B, Faka S, Pareek V, et al. Simulations and optimization of a reduced CO 2 emission process for methanol production using syngas from bi-reforming. Energy Fuels 2021;35(10):8844–56. https://doi.org/10.1021/acs.energyfuels.1c00227.

[12] Chein R-Y, Chen W-H, Chyuan Ong H, Loke Show P, Singh Y. Analysis of methanol synthesis using CO2 hydrogenation and syngas produced from biogas-based reforming processes. Chem Eng J 2021;426:130835. https://doi.org/10.1016/j.cej.2021.130835.

[13] Hernandez B, Martin M. Optimization for biogas to chemicals via tri-reforming. Analysis of Fischer-Tropsch fuels from biogas. Energ Conver Manage 2018;174:998–1013. https://doi.org/10.1016/j.enconman.2018.08.074.

[14] Chein R-Y, Hsu W-H. Analysis of syngas production from biogas via the tri-reforming process. Energies 2018;11(5):1075. https://doi.org/10.3390/en11051075.

[15] Farsi M, Lari MF. Methanol production based on methane tri-reforming: Process modeling and optimization. Process Saf Environ Prot 2020;138:269–78. https://doi.org/10.1016/j.psep.2020.03.014.

[16] Zhang Y, Cruz J, Zhang S, Lou HH, Benson TJ. Process simulation and optimization of methanol production coupled to tri-reforming process. Int J Hydrogen Energy 2013;38(31):13617–30. https://doi.org/10.1016/j.ijhydene.2013.08.009.

[17] Lim D, Lee B, Lee H, Byun M, Lim H. Projected cost analysis of hybrid methanol production from tri-reforming of methane integrated with various water electrolysis systems: Technical and economic assessment. Renew Sustain Energy Rev 2022;155:111876. https://doi.org/10.1016/j.rser.2021.111876.

[18] Choe C, Byun M, Lee H, Lim H. Techno-economic and environmental assessments for sustainable bio-methanol production as landfill gas valorization. Waste Manag 2022;150:90–7. https://doi.org/10.1016/j.wasman.2022.06.040.

[19] Moioli E, Schildhauer T. Eco-techno-economic analysis of methanol production from biogas and power-to-X. Ind Eng Chem Res 2022;61(21):7335–48. https://doi.org/10.1021/acs.iecr.1c04682.

[20] Sens L, Piguel Y, Neuling U, Timmerberg S, Wilbrand K, Kaltschmitt M. Cost minimized hydrogen from solar and wind – Production and supply in the European catchment area. Energ Conver Manage 2022;265:115742. https://doi.org/10.1016/j.enconman.2022.115742.

[21] aspentech. Aspen Plus.

[22] Association for the Advancement of Cost Engineering. COST ESTIMATE CLASSIFICATION SYSTEM-AS APPLIED IN ENGINEERING, PROCUREMENT, AND CONSTRUCTION FOR THE PROCESS INDUSTRIES: AACE® International Recommended Practice No. 18R-97. TCM Framework: 7.3 – Cost Estimating and Budgeting.

[23] Zhao X, Joseph B, Kuhn J, Ozcan S. Biogas reforming to syngas: A review. iScience 2020;23(5):101082. https://doi.org/10.1016/j.isci.2020.101082.

[24] Wismann ST, Engbæk JS, Vendelbo SB, Bendixen FB, Eriksen WL, Aasberg-Petersen K, et al. Electrified methane reforming: A compact approach to greener industrial hydrogen production. Science 2019;364(6442):756–9. https://doi.org/10.1126/science.aaw8775.

[25] Danish Energy Agency. Technology Data for Industrial Process Heat: Datasheet for industrial process heat. [September 06, 2023]; Available from: https://ens.dk/en/our-services/projections-and-models/technology-data/technology-data-industrial-process-heat.

[26] Topsoe. eREACT™ Fuels: New technology essential for electrofuels production. [December 19, 2023]; Available from: https://www.topsoe.com/our-resources/knowledge/our-products/equipment/e-react-fuels.

[27] BASF. BASF, SABIC und Linde beginnen mit dem Bau der weltweit ersten Demonstrationsanlage für großtechnische elektrisch beheizte Steamcracker-Öfen. [19/12.2023]; Available from: https://www.basf.com/global/de/media/news-releases/2022/09/p-22-326.html.

[28] Hiller H, Reimert R, Marschner F, Renner H-J, Boll W, Supp E et al. Gas Production. In: Ullmann's Encyclopedia of Industrial Chemistry.

[29] Ciambelli P. 2 Catalytic autothermal reforming for hydrogen production: from large-scale plant to distributed energy system. In: van de Voorde M, editor. Hydrogen Production and Energy Transition. De Gruyter; 2021, p. 171–192.

[30] Kaltschmitt M, Hartmann H, Hofbauer H (eds.). Energie aus Biomasse: Grundlagen, Techniken und Verfahren. 3rd ed. Berlin: Springer Vieweg; 2016.

[31] Fachagentur Nachwachsende Rohstoffe e. V. Nachwachsende Rohstoffe: Basisdaten Bioenergie Deutschland 2022; 2023.

[32] Vita A, Italiano C, Previtali D, Fabiano C, Palella A, Freni F, et al. Methanol synthesis from biogas: A thermodynamic analysis. Renew Energy 2018;118:673–84. https://doi.org/10.1016/j.renene.2017.11.029.

[33] Buttler A, Spliethoff H. Current status of water electrolysis for energy storage, grid balancing and sector coupling via power-to-gas and power-to-liquids: A review. Renew Sustain Energy Rev 2018;82:2440–54. https://doi.org/10.1016/j.rser.2017.09.003.

[34] Jang W-J, Jeong D-W, Shim J-O, Kim H-M, Roh H-S, Son IH, et al. Combined steam and carbon dioxide reforming of methane and side reactions: Thermodynamic equilibrium analysis and experimental application. Appl Energy 2016;173:80–91. https://doi.org/10.1016/j.apenergy.2016.04.006.

[35] König DH. Techno-ökonomische Prozessbewertung der Herstellung synthetischen Flugturbinentreibstoffes aus CO2 und H2; 2016.

[36] Mbatha S, Everson RC, Musyoka NM, Langmi HW, Lanzini A, Brilman W. Power-to-methanol process: a review of electrolysis, methanol catalysts, kinetics, reactor designs and modelling, process integration, optimisation, and techno-economics. Sustain Energy Fuels 2021;5(14):3490–569. https://doi.org/10.1039/D1SE00635E.

[37] Butera G, Fendt S, Jensen SH, Ahrenfeldt J, Clausen LR. Flexible methanol production units coupling solid oxide cells and thermochemical biomass conversion via different gasification technologies. Energy 2020;208:118432. https://doi.org/10.1016/j.energy.2020.118432.

[38] M. Dreher, M. Memmler, S. Rother, S. Schneider. Bioenergie - Datengrundlagen für die Statistik der erneuerbaren Energien und Emissionsbilanzierung: Ergebnisbericht zum Workshop vom Juli 2011; 2011.

[39] Fasihi M, Breyer C. Baseload electricity and hydrogen supply based on hybrid PV-wind power plants. J Clean Prod 2020;243:118466. https://doi.org/10.1016/j.jclepro.2019.118466.

[40] Towler GP, Sinnott RK. Chemical engineering design: Principles, practice, and economics of plant and process design. 2nd ed. Boston MA: Butterworth-Heinemann; 2013.

[41] Peters MS, Timmerhaus KD, West RE. Plant design and economics for chemical engineers. 5th ed. Boston: McGraw-Hill; 2006.

[42] Martin Wietschel. Klimabilanz, Kosten und Potenziale verschiedener Kraftstoffarten und Antriebssysteme für Pkw und Lkw: Endbericht 2019. Doi: 10.24406/publica-fhg-299856.

[43] Umweltbundesamt. Optionen für Biogas-Bestandsanlagen bis 2030 aus ökonomischer und energiewirtschaftlicher Sicht: Abschlussbericht; 2020.

[44] Eurostat. Electricity prices for non-household consumers - bi-annual data (from 2007 onwards): Online data code: nrg_pc_205; Available from: https://ec.europa.eu/eurostat/databrowser/view/nrg_pc_205/default/table?lang=en.

[45] Boulamanti A, Moya JA. Production costs of the chemical industry in the EU and other countries: Ammonia, methanol and light olefins. Renew Sustain Energy Rev 2017;68:1205–12. https://doi.org/10.1016/j.rser.2016.02.021.

[46] EEA E. Preisentwicklung von CO2-Emissionsrechten im europäischen Emissionshandel (EU-ETS) von 2005 bis 2022. [November 03, 2023]; Available from: https://de.statista.com/statistik/daten/studie/1304069/umfrage/preisentwicklung-von-co2-emissionsrechten-in-eu/.

[47] Svanberg M, Ellis J, Lundgren J, Landälv I. Renewable methanol as a fuel for the shipping industry. Renew Sustain Energy Rev 2018;94:1217–28. https://doi.org/10.1016/j.rser.2018.06.058.

[48] Kajaste R, Hurme M, Oinas P. Methanol-Managing greenhouse gas emissions in the production chain by optimizing the resource base. AIMS Energy 2018;6(6):1074–102. https://doi.org/10.3934/energy.2018.6.1074.